

# OVERVIEW OF ARC OPTICS OF FCC-hh

A. Chance\*, D. Boutin, B. Dalena

CEA, IRFU, DACM, Université Paris-Saclay, F-91191 Gif-sur-Yvette, France

B. Holzer, D. Schulte, CERN, Geneva, Switzerland

## Abstract

The FCC-hh (Future Hadron-Hadron Circular Collider) is one of the options considered for the next generation accelerator in high-energy physics as recommended by the European Strategy Group. In this overview the status and the evolution of the design of optics integration of FCC-hh are described, focusing on design of the arcs, alternatives, and tuning procedures.

## LAYOUT OF THE FCC-hh

The layout of the FCC-hh ring is shown in Fig. 1. It has only slightly changed compared to the one shown in Ref. [1]. The total circumference of the FCC-hh ring is 97.75 km. The FCC-hh ring is made of 4 short arcs (SAR), 4 long arcs (LAR), 6 long straight sections of 1.4 km (LSS) and 2 extended straight sections of 2.8 km (ESS). The parameters of the ring are given in Table 1.

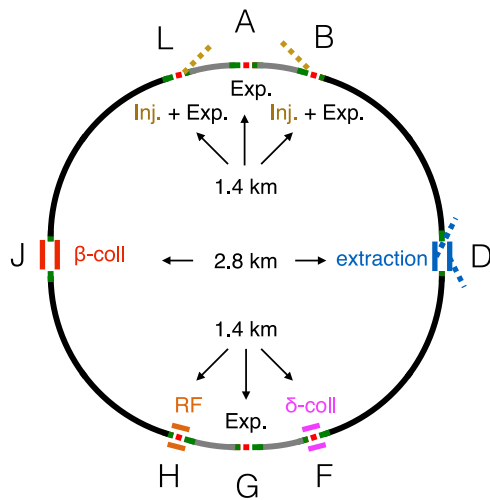


Figure 1: Layout of the FCC-hh ring.

The high luminosity interaction points (IPs) are located in the sections LSS-PA and LSS-PG. The value of  $L^*$  in the experimental insertion region (EIR) has been shortened from 45 m to 40 m [2–4], giving a greater flexibility to the optics and reducing the chromaticity generated into the triplet. Two additional IPs (with lower luminosity) are located in the sections LSS-PB and LSS-PL. These sections host the injection as well, which gives additional constraints [2, 4, 5]. The beam H1, which runs in the clockwise direction, is injected into the section LSS-PB and the other one H2 into the section LSS-PL. The RF cavities are located into the section LSS-PH with a beam separation enlarged from 204 mm

\* Corresponding author: antoine.chance@cea.fr

Table 1: Parameters of the FCC-hh Ring

Parameter	Value		Unit
	Baseline	Ultimate	
Energy	50		TeV
Circumference	97.75		km
LSS and ESS length	1.4 and 2.8		km
SAR and LAR length	3.4 and 16		km
$\beta^*$	1.1	0.3	m
$L^*$	40		m
Normalized emittance	2.2		$\mu\text{m}$
$\gamma_{\text{tr}}$	98.806	98.802	
$Q_x/Q_y$	110.31/ 107.32		
$Q'_x/Q'_y$	2/2		
Beam separation	204		mm
Beam separation (RF)	420		mm

to 420 mm. This section is currently made of FODO cells. The extraction section is located in the section ESS-PD and enables the extraction of both beams in the same section [5]. The betatron cleaning section is located in the section ESS-PJ for both beams. The momentum cleaning section is located in the section LSS-PF for both beams [6–8].

## UPDATES OF THE ARC CELLS

To reduce the cost and to enable the compatibility between FCC-hh and HE-LHC, the beam separation is 204 mm [9, 10]. Because of the strong magnetic field in the dipoles, the yoke saturates at collision energy and creates a quadrupole component. The dipoles have then a systematic  $b_2$  component, which increases from injection (near 0) to collision energy (near 50 units). Moreover, the sign of  $b_2$  is inverted between the inner and outer sides of the arcs for the cos  $\theta$  or block designs. For the beam H1, we consider then  $b_2 = 50$  from PA to PB and from PG to PL and  $b_2 = -50$  in the other sections. For the beam H2, the signs are inverted. The integrated quadrupole component in a dipole is given by:

$$\frac{b_2 L_d}{\rho R_{\text{ref}}} \approx 0.4 \times 10^{-3} \quad (1)$$

where  $L_d$  and  $\rho$  are respectively the length and the curvature radius of the dipole,  $R_{\text{ref}} = 17$  mm is the reference radius. For comparison, the integrated gradient in one arc quadrupole is about  $14 \times 10^{-3}$ . Since there are 12 dipoles and 2 quadrupoles per cell, the integrated gradient in the dipoles is equal to 17% of the one in the main quadrupoles, which is not negligible. That is why the  $b_2$  component of the dipoles is not considered as a perturbation and is taken into account



Content from this work may be used under the terms of the CC BY 3.0 licence (© 2018). Any distribution of this work must maintain attribution to the author(s), title of the work, publisher, and DOI.

in the arc design. A direct consequence of  $b_2$  is an imbalance between maxima of the horizontal and vertical betatron functions because the dipoles are focusing or defocusing when  $b_2$  is positive or negative. The current arc quadrupole is with 2 layers against 4 layers in Ref. [1], which reduces the maximum gradient from 380 T/m to 360 T/m [11]. The quadrupoles were then lengthened from 6 m to 7.2 m to compensate the integrated gradient of the dipoles and the smaller gradient.

The layouts of the arc half-cell, of the short straight section, and of the dispersion suppressor (DIS) are given in Fig. 2. Each FODO cell has 12 dipoles, 12  $b_3$  correctors (MCS), and 2 short straight sections (SSS). Each SSS contains one BPM, one sextupole, one quadrupole, one multipole corrector (trim quadrupole, skew quadrupole, or octupole), and one dipole corrector. The length of these magnets are optimized accordingly with the reachable maximum gradients [12,13]. The total length of the SSS is 12.0 m. The distances between elements of the arc cell is summarized in Table 2. The DIS are similar to the ones used in LHC [14]. Like in HL-LHC, some space (5 meters) is saved for two 1-meter-long collimators to protect the arc entrances from the debris coming from the insertions (mainly experimental and cleaning ones [15]). The optical functions and the geometrical apertures in the arc cell baseline (with  $b_2 = \pm 50$  unit in the dipoles) are shown in Fig. 3. The beam stay clear was computed with the last version of the beam screen [16] and taking into account the dipole sagitta and the misalignment tolerances [15].



Figure 2: Layout of the arc FODO half-cell and DIS

## OPTICS OF THE FCC-hh RING

The optics of the different main insertions are given in Fig. 4 for the ultimate parameters given in Table 1. The

Table 2: Parameters of the Arc FODO Cell

Parameter	Value	Unit
Cell length	213.03	m
Cell phase advance H/V	90	deg
Number of dipoles per cell	12	
Dipole magnetic length	14.069	m
Dipole maximum field	15.96	T
Quadrupole magnetic length	7.2	m
Quadrupole maximum gradient	360	T/m
Sextupole magnetic length	1.2	m
Sextupole maximum gradient	3724/7000	T/m <sup>2</sup>
Baseline/Ulimate		
Distance MB-MB	1.5	m
Distance MB-SSS	1.3	m
Distance MQ-other	0.35	m
Distance other-other	0.35	m

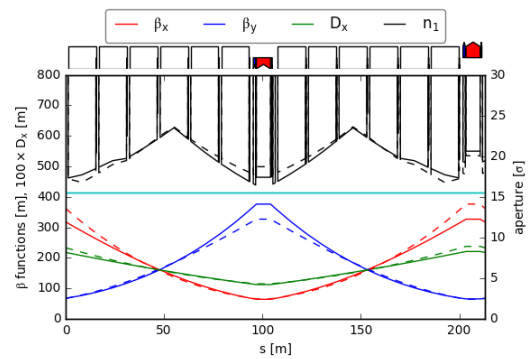


Figure 3: Optical functions ( $\beta_x$  in red,  $\beta_y$  in blue and  $D_x$  in green) in the FODO cell in the case of  $b_2 = 50$  (full line) and  $b_2 = -50$  (dashed line). The physical aperture in  $\sigma$  at injection energy of 3.3 TeV is shown in black. The target aperture of  $15.5 \sigma$  is plotted in cyan.

current parameters of the FODO cell are summed up in Table 2. Two tuning procedures can be used for the arc optics. In one case, the phase advances in the FODO cells are exactly  $90^\circ$  in the SAR whereas they are  $90 + \epsilon_{x,y}^\circ$  in the LAR. The value of  $\epsilon_{x,y}$  is adjusted to tune the whole ring. The large number of FODO cells in the LAR enables to keep the value of  $\epsilon_{x,y}$  small. In the second case, phase trombones are inserted at PD and PJ to adjust the working point and the phase advance between PA and PG. Indeed, studies have shown that the dynamic aperture and machine stability are very sensitive to this value [17, 18]. To scan the phase advances, this method was more straightforward than using the former tuning procedures. Obviously, when these phase advances are frozen, the collider optics is tuned with the first method. An alternative is to tune the insertions LSS-PH, hosting the RF, and the extraction section ESS-PD but this method has not been implemented yet.

Currently, a dipole is removed at the middle of the LAR to save some space for the technical straight sections (TSS). Because of the  $b_2$  in the dipoles, removing another dipole

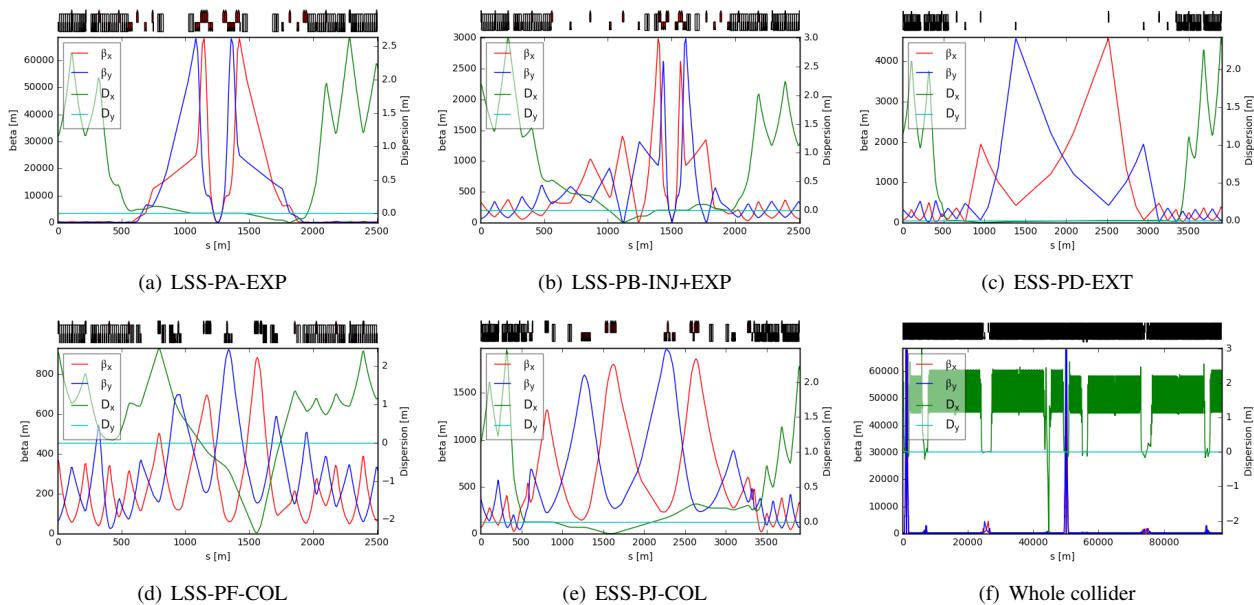


Figure 4: Optical functions of the insertion regions at collision: high-luminosity IR, low-luminosity IR with injection, extraction section, betatron and momentum collimation section.

two FODO cells downstream [1] cannot work any more. The current solution is to use 2 sets of 4 trim quadrupoles (separated each by one FODO cell). The 2 sets are separated by one half FODO cell. By this way, it is possible to correct the dispersion wave and the betatron wave. The residual betatron wave is then a few percent's against 15% before. However, the studies on the civil engineering show that removing this dipole may not be needed (the technical straight sections would be situated in a separated cavern and do not require a long drift in the lattice any more). Currently, the chromaticity is corrected by two sextupole families distributed in the SAR and LAR. More advanced schemes will be studied in the future when the first order optics is frozen.

Correction schemes are explained in Ref. [17, 19] and will not be developed here. The SSC scheme is used with trim or skew quadrupole at the arc entrance in order to correct the spurious dispersion coming from the EIR [1, 20].

## ALTERNATIVES

The current inner triplet is made of a set of 2-4-2 quadrupole units of different lengths. There is an alternative triplet which uses the same length of quadrupoles with a configuration of 2-3-2 quadrupole units. This configuration works also with a flat optics with no crab cavities ( $\beta_x^* = 0.15$  m and  $\beta_y^* = 1.2$  m), which is an alternative to the ultimate optics [21].

An alternative to the arc optics is to use phase advances of  $60^\circ$  instead of  $90^\circ$  in the arc cells. The motivation is to reduce the needed integrated quadrupole gradient, to use shorter quadrupoles, and finally to use longer and weaker dipoles. By keeping a maximum gradient of 360 T/m, the quadrupoles can be shortened from 7.2 m to 5.4 m; the

dipoles can be lengthened by 0.3 m and the dipole field can be reduced to 15.61 T. Another advantage is to reduce the maximum sextupole gradient thanks to larger dispersion functions. The maximum sextupole gradient is then 3300 T/m<sup>2</sup> for the ultimate lattice. Nevertheless, the correction schemes should be modified to work with this phase advance. The main issue is the reduction of the physical aperture at injection because of enlarged dispersion. At injection energy of 3.3 TeV, the physical aperture is only  $12.5\sigma$ , well below the target limit of  $15.5\sigma$ .

## CONCLUSION

An updated status of the optics of the FCC-hh ring has been given. The impact of the  $b_2$  component of the main dipoles has been commented. The layout of the arc cell has been shown and has been updated in agreement with magnet specifications. The geometric aperture is within requirements. Alternatives have been discussed.

## ACKNOWLEDGEMENTS

The European Circular Energy-Frontier Collider Study (EuroCirCol) project has received funding from the European Union's Horizon 2020 research and innovation programme under grant No 654305. The information herein only reflects the views of its authors and the European Commission is not responsible for any use that may be made of the information.

## REFERENCES

- [1] A. Chancé *et al.*, "Updates on the Optics of the Future Hadron-Hadron Collider FCC-hh," in *Proceedings of the 8th Interna-*

- Content from this work may be used under the terms of the CC BY 3.0 licence (© 2018). Any distribution of this work must maintain attribution to the author(s), title of the work, publisher, and DOI.
- tional Particle Accelerator Conference (IPAC 2017)*, Copenhagen, Denmark, May 14-19, 2017, p. TUPVA002, 2017.
- [2] A. Seryi *et al.*, “Overview of Design Development of FCC-hh Experimental Interaction Regions,” in *Proceedings, 8th International Particle Accelerator Conference (IPAC 2017)*, Copenhagen, Denmark, May 14-19, 2017, p. TUPVA040, 2017.
- [3] A. Seryi, “Preliminary EIR design baseline: Deliverable D3.2,” Tech. Rep. EuroCirCol-P2-WP3-D3.2, CERN, Geneva, November 2017.
- [4] R. Martin *et al.*, “Experimental Insertions.” presented at FCC week 2018, Amsterdam, Netherlands, April 2018, unpublished.
- [5] E. Renner *et al.*, “FCC-hh injection and extraction: insertions and requirements.” presented at FCC week 2018, Amsterdam, Netherlands, April 2018, unpublished.
- [6] J. Molson *et al.*, “Status of the FCC-hh Collimation System,” in *Proceedings, 8th International Particle Accelerator Conference (IPAC 2017)*, Copenhagen, Denmark, May 14-19, 2017, p. MOPAB001, 2017.
- [7] J. Molson *et al.*, “A Comparison of Interaction Physics for Proton Collimation Systems in Current Simulation Tools,” in *Proceedings, 8th International Particle Accelerator Conference (IPAC 2017)*, Copenhagen, Denmark, May 14-19, 2017, p. WEOBA1, 2017.
- [8] J. Molson *et al.*, “Betatron collimation system insertions.” presented at FCC week 2018, Amsterdam, Netherlands, April 2018, unpublished.
- [9] V. Marinozzi *et al.*, “Conceptual Design of a 16 T  $\cos \theta$ ; Bending Dipole for the Future Circular Collider,” *IEEE Transactions on Applied Superconductivity*, vol. 28, pp. 1–5, April 2018.
- [10] C. Lorin, M. Segreti, and M. Durante, “Design of a Nb3Sn 16 T Block Dipole for the Future Circular Collider,” *IEEE Transactions on Applied Superconductivity*, vol. 28, pp. 1–5, April 2018.
- [11] C. Lorin, “FCC Main Quad.” presented at FCC week 2018, Amsterdam, Netherlands, April 2018, unpublished.
- [12] D. Schoerling *et al.*, “Other magnets parameters.” presented at FCC week 2018, Amsterdam, Netherlands, April 2018, unpublished.
- [13] A. Chance, “Preliminary arc design baseline: Deliverable D2.4,” Tech. Rep. EuroCirCol-P2-WP2-D2.4, CERN, Geneva, November 2017.
- [14] A. Chance *et al.*, “First results for a FCC-hh ring optics design,” Tech. Rep. CERN-ACC-2015-0035, CERN, Geneva, Apr 2015.
- [15] R. Bruce *et al.*, “Status of FCC-hh collimation studies.” presented at FCC week 2018, Amsterdam, Netherlands, April 2018, unpublished.
- [16] F. Perez *et al.*, “FCC-hh beam vacuum concept: design, tests and feasibility.” presented at FCC week 2018, Amsterdam, Netherlands, April 2018, unpublished.
- [17] B. Dalena *et al.*, “Dipole Field Quality and Dynamic Aperture for FCC-hh,” presented at IPAC2018, Vancouver, BC, Canada, paper MOPMF024, this conference.
- [18] E. Cruz-Alaniz *et al.*, “Methods to Increase the Dynamic Aperture of the FCC-hh Lattice,” presented at IPAC2018, Vancouver, BC, Canada, paper THPAK145, this conference.
- [19] D. Boutin *et al.*, “Updates on the Optics Correction of the FCC-hh,” presented at IPAC2018, Vancouver, BC, Canada, paper MOPMF023, this conference.
- [20] Y. Nosochkov and D. M. Ritson, “The provision of IP crossing angles for the SSC,” in *Proceedings of International Conference on Particle Accelerators*, pp. 125–127 vol.1, May 1993.
- [21] J. Abelleira *et al.*, “FCC-hh Final-Focus for Flat-Beams: Parameters and Energy Deposition Studies.” presented at FCC week 2018, Amsterdam, Netherlands, April 2018, unpublished.